

AC field induced two-dimensional aggregation of multilamellar vesicles

C. Faure, N. Decoster, and F. Argoul^a

Centre de Recherche Paul Pascal, avenue A. Schweitzer, 33600 Pessac, France

Received: 4 December 1997 / Revised: 24 March 1998 / Accepted: 4 May 1998

Abstract. The aggregation of 2D colloidal crystals can be performed by applying an AC field to a colloidal dispersion. This technique is used in this work for assembling multilamellar vesicles in suspension. The dynamics of the aggregation is followed by real-time recording of the pictures of the microsphere assembly through a phase contrast microscope. The influence of both the frequency and the amplitude of the alternating field on the dynamical evolution of the concentration of layered particles is discussed with respect to their size. A phenomenological model of double layer induced trapping of the particles is proposed and an electroconvective instability of the fluid surrounding the particles is suggested from the observation of the local dynamics of the particles, in accordance with a very recent argument of Yeh *et al.* [1].

PACS. 05.70.Fh Phase transitions: general aspects – 83.70.Hq Heterogeneous liquids: suspensions, dispersions, emulsions, pastes, slurries, foams, block copolymers, etc.

1 Introduction

The possibility of forming two-dimensional colloidal crystals of microscopic size has attracted the interest of physicists since the early eighties for the modeling of two dimensional phase transitions [2,3] and for their potential applications in micro-electronics and optics [4]. Two different types of methods have been used to tune the interaction forces between colloidal particles. The first one consists in confining the spheres at the air-water interface [5], either by drying a thin layer of water in which the colloidal particles are dispersed [2,6–8] or by assembling latex spheres by van der Waals or capillary forces at the water/air interface [3,5,9,10]. The second one is driven by the electrostatic interactions between a charged solid substrate and the particles. This surface charge can be produced either by the deposition of a monolayer film on the substrate [4,11], the suspension fluid is then drained either by spin-coating [4] or by a dipping technique [11], or by imposing an electric polarization (DC or AC) at the electrode/electrolyte interface [1,12–15]. We will focus on this last technique in this paper. During the past ten years there have been few attempts for interpreting the type of interactions which are involved in the second system [1,12,14,15]. Despite the various studies of electrokinetic phenomena which have focused on colloidal suspensions since the seventies [16–18], it is only very recently that the question of the origin of the attractive interaction between particles which builds such crystal phases has been addressed. In a very recent work, Yeh *et al.* [1] brought for

the first time a sketch of an electrohydrodynamic instability of the fluid between neighbouring particles to explain the long range attractive interaction introduced by the AC field. The detailed characterization of transport dynamics of both the particles and the surrounding fluid is a fundamental issue for the validation of such mechanism.

In the present paper we apply an AC electric field to initiate the two dimensional aggregation of multilamellar vesicles also called spherulites or onions, dispersed in water. These spherulites have been obtained by shearing a lyotropic lamellar phase [19,20] and own the definite advantage, over standard systems such as plain polymeric or metal spheres, of allowing the encapsulation of various chemicals either in the aqueous phase or in the lamellar phase according to their hydrophilicity. In a recent work [21,22], they have been used as microreactors for the synthesis of metal microspheres. The primary objective of this work is to show that these multilamellar microsystems can be assembled in a two dimensional layer by applying an AC field. The originality of our approach is based both on the choice of the colloidal suspensions, and on the analysis of the local dynamics of the assembling process. In the second section, we describe the preparation of the spherulites together with the experimental setup and protocole. In the third section we analyze the aggregation process and the time evolution of the number of assembled particles, when the AC field is set on and off. We discuss thereby the different forces involved in the particle/particle and particle/electrode interactions and their respective dependence on the electrical parameters (electric field intensity and frequency).

^a e-mail: argoul@crpp.u-bordeaux.fr

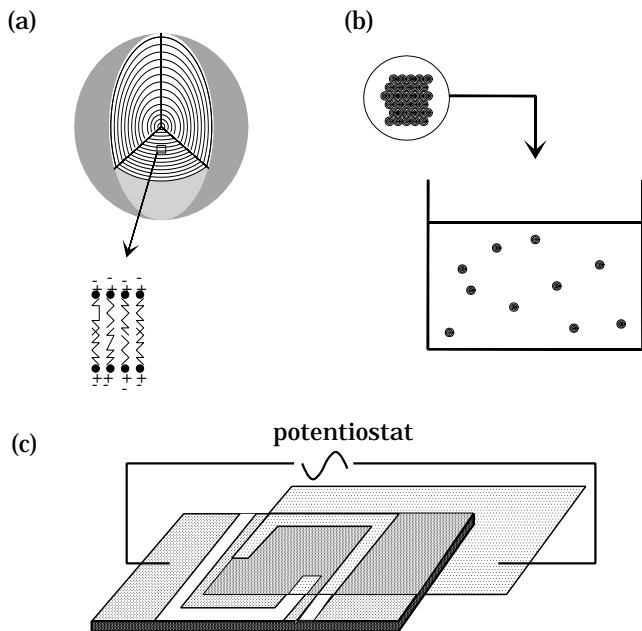


Fig. 1. Experimental aspects. (a) Schematic representation of the multilamellar structure of a spherulite. (b) Compact spherulite phase and its dispersion in water. (c) Sketch of the micro-cell.

2 Experimental set-up

2.1 Preparation of the spherulites

Multilamellar vesicles, also called spherulites, are usually prepared by the shearing in a Couette cell of a lamellar phase without excess solvent [19,20]. For some systems and for ours particularly, the spherulites can be obtained by a manual shearing of the lamellar phase. The lamellar phase is obtained by mixing 40%w of Genamin T-020 (Hoechst, Frankfurt, Germany) with 60%w of a copper sulphate solution ($\text{CuSO}_4 \cdot 5\text{H}_2\text{O}$ (11%w) Aldrich, Steinheim, Germany). It is manually sheared for *ca.* 10 minutes and then left for 10 additional minutes. This operation is repeated until the sample reaches an homogeneous blue colour. This recipe leads to the formation of a compact phase of multilamellar vesicles, such as drawn in Figure 1a, which can be observed by phase contrast microscopy since their size distributions determined by laser diffraction show that their diameters range from $0.06 \mu\text{m}$ to $3 \mu\text{m}$ [21]. This compact phase is metastable and can be kept in its state for weeks. When this phase is dispersed in water (Fig. 1b), the spherulites are submitted to osmotic pressure gradients and their metastability can be drastically reduced. In our case, the choice of copper ion doped Genamin T-020 is the key ingredient which improves the stability of spherulites when dissolved in water [21,22]. For all experiments, the concentration in spherulites in the water dispersion is 5.2 mg/ml .

The choice of a manual shearing, despite the fact that it cannot attain the monodispersity which can be reached with a Couette cell, has been preferred in this first study because it does not involve any sophisticated rheophysics

device [19,20] and can therefore be reproduced with little technical means. Moreover, in our analysis the polydisperse character of the particle dispersion is interesting since it sheds light on the local fluid dynamics and it also provides some insight on the size dependence of the assembly process.

2.2 Experimental cell

The experimental cell is sketched in Figure 1c, it consists of two glass slides which, after being washed in sulphochromic acid (SDS, Peypin, France), are covered by a thin layer of gold by sublimation under vacuum (MED010 Balzers Union). The two glass slides are sealed together by a silicone joint (CAF4, Rhône Poulenc, France), with their conducting sides facing each other. The silicone joint is cut according to a predefined mask to let two apertures by which the suspension of spherulites can be introduced. The interspace between the glass slides, defined by the silicone joint, is *ca.* $200 \mu\text{m}$, and its area 1 cm^2 . Once the cell is filled with the colloidal suspension, the two apertures are sealed with CAF4. The two gold-film electrodes are connected by a copper thread to a generator (Hewlett Packard, 3324A). In this configuration the electrical field is applied normally to the glass slides.

2.3 Data recording and treatment

The observation of the spherulite suspension is performed through a phase-contrast microscope (IM35) with an oil-immersion objective ($\times 100/1.25$ Zeiss, Oberkochen, Germany) and recorded by a CCD video camera (C2400-77, Hamamatsu, Japan) on a U-matic video recorder (VO 5630, Sony, Japan). The video tapes are further digitized into stacks of 768×512 pixel images by a frame grabber and data acquisition software [23]. Further treatments such as image filtering and contour detection are performed on a HP7000 station.

3 AC field induced aggregation of spherulites

In our study, we have chosen copper ion doped spherulites for their stability and the simplicity of their fabrication by a manual shearing. The fact that they are “physical” objects with comparison to polymer beads obtained by a chemical synthesis must be outlined before entering the precise description of our AC field experiments. Indeed, their mode of preparation does not lead to irreversible objects, since when dispersed in water they are progressively stripped of their outer bilayers and they loose their spherical compact structure within a few days. The stability of these spherulites, when submitted to an AC field remains therefore a key interrogation that will only be suggested in this study. In this paper, we show for the first time that there exists a range of frequency ($0.5 \text{ kHz} \sim 50 \text{ kHz}$) in which the application of an AC field to a spherulite dispersion can lead to an aggregation of these spherical objects on the surface of a planar electrode, very much like

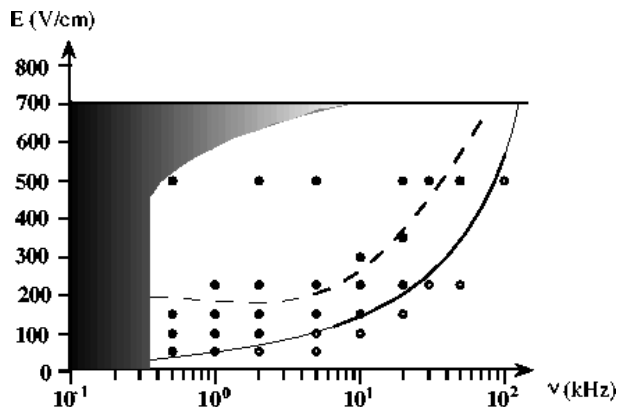


Fig. 2. Two dimensional $(\nu, |E|)$ phase diagram showing the zone of existence of the assembly process. The dark points correspond to experiments where a notable assembling has been observed within one hour. The black circles above the dashed line correspond to a fast assembling process (which could not be resolved in time by our frame grabber). On the left side of the diagram the hashed zone corresponds to the zone of instability of the spherulites. The field amplitude is bounded to 700 V/cm by experimental limitations.

preceding observations on latex and metal particle dispersions [1, 12–15]. Moreover, this process is reversible since particles return to the bulk water when the electric field is turned off. This provides evidence for the electrostatic nature of the interaction of the spherulites with the electrode at these frequencies and rules out chemical or electrochemical interactions (chemical adsorption or charge transfer). We observe, as expected, a strong asymmetry of the dynamics of aggregation and redispersion of the spherulites when the AC field is turned on and off, since the aggregation process depends on the electric field, whereas the dispersion process is independent of it. We propose in this paper to focus on the dynamics of aggregation and redispersion to get a more precise picture on the interaction forces between the particles and to discuss the influence of the amplitude and the frequency of the electric field on the assembling process.

3.1 Experimental observations

3.1.1 Description of the assembling process and its dynamical characteristics

In the experiments reported here, dispersions of spherulites are submitted to an AC field (E) whose amplitude varies from 50 V/cm to 500 V/cm and frequency (ν) ranges from 0.2 kHz to 100 kHz. Figure 2 reports a phase diagram (ν, E) where the zones of existence of assembling are delimited. The black circles correspond to experiments where the initially dispersed spherulites are symmetrically attracted by both electrodes. Once trapped closely to the interface, they do not stay steady but they reorganize along the surface of the electrode to optimize the filling of this two-dimensional space by a complex alternance of big and small spherulites forming patchy ag-

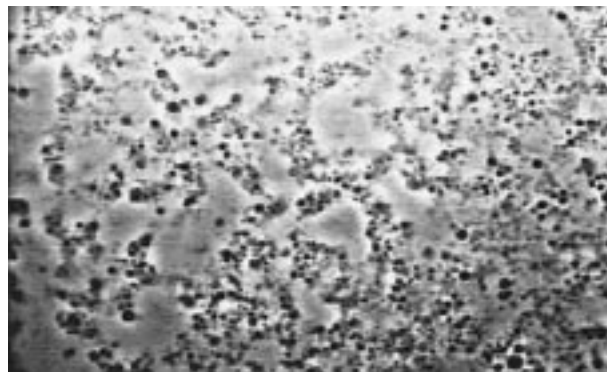


Fig. 3. Picture of the assembled layer of spherulites. Amplitude of the AC field 150 V/cm, frequency $\nu = 1$ kHz. Length of the figure 150 μm .

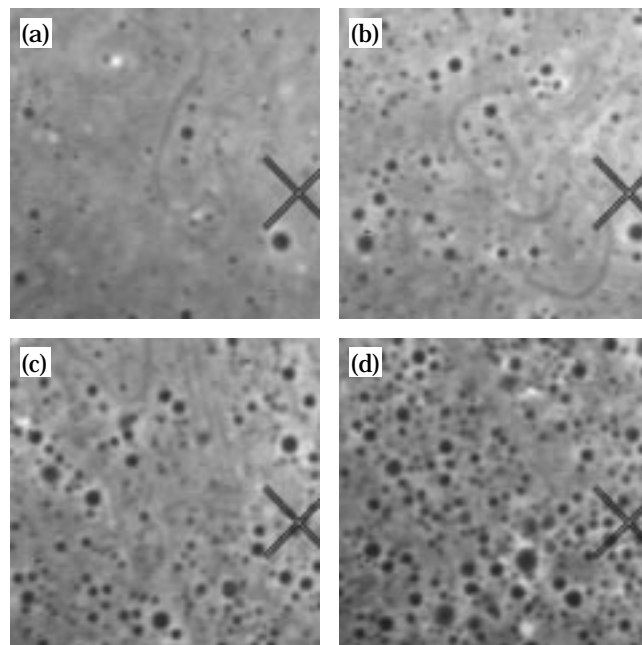


Fig. 4. AC field induced aggregation of multilamellar spherulites including copper sulphate solution, time evolution of the structured pattern. AC field amplitude 150 V/cm, frequency 1 kHz, $[\text{CuSO}_4] = 1.3 \times 10^{-3}$ M inside the spherulites. (a) $t = 0$ s, (b) $t = 30$ s, (c) $t = 2$ min, (d) $t = 7$ min. Width of the pictures 30 μm .

gregated zones, separated by empty zones as illustrated in Figure 3. These empty zones indicate the implication of a longer range attractive force between the particles (with respect to their dipolar electrostatic repulsion). This assembled layer of spherulites sits at a finite distance to the electrode of the order of a micron. In our case, gravity forces do not play a major role during the aggregation process because once the field is turned off, the layer of spherulites on the bottom electrode totally redisperses in the bulk in a few minutes. These multilamellar vesicle dispersions are therefore shown to behave quite similarly to latex dispersions where such assembling processes were previously reported in the literature [1, 12, 14].

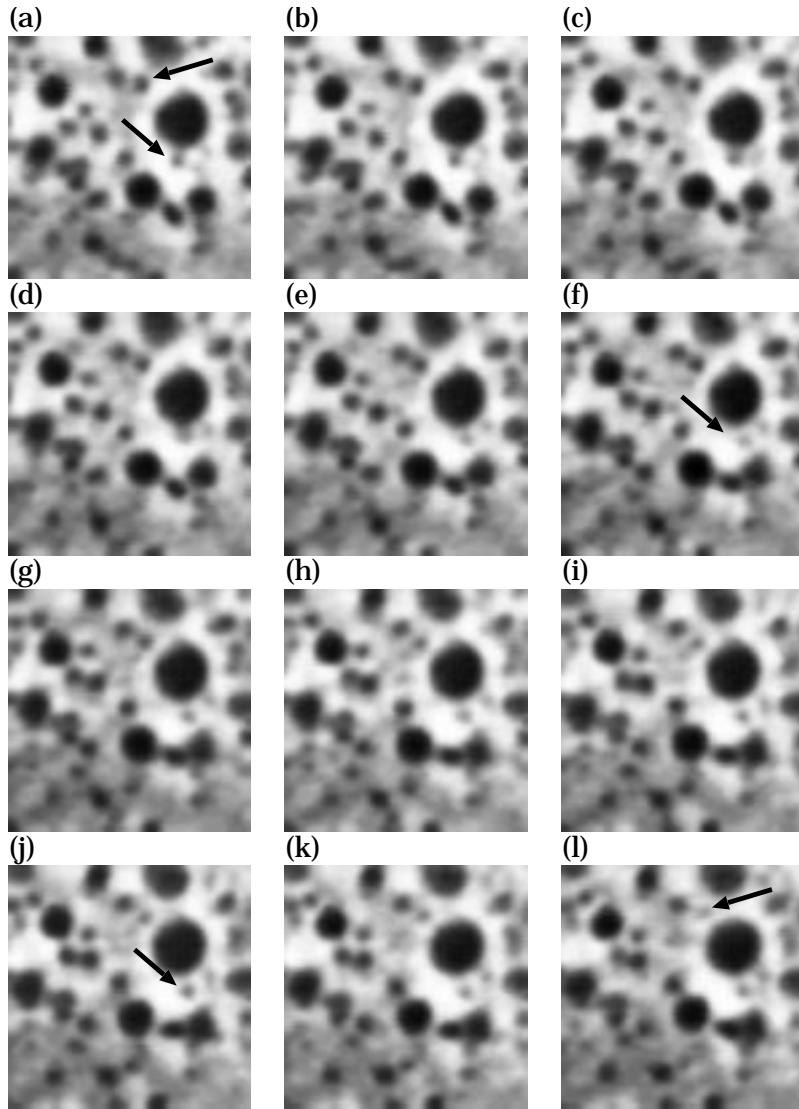


Fig. 5. Local dynamics of the aggregated spherulites. The time interval between successive pictures is $\Delta t = 0.04$ s, AC field 150 V/cm, frequency 1 kHz. The darkness of the particles is related to their position with respect to the confocal plane, their turning grey is related to their escape from the focal plane of the microscope objective. Width of the pictures 10 μm .

In Figure 4 we report four successive pictures of the aggregation of the spherulites, obtained for an AC field amplitude of 150 V/cm and frequency of 1 kHz. In this set of pictures, we focus on a small sub-region of an aggregated zone. Around each big sphere a brighter zone exists which remains quite free of spherulites in average, if one smaller sphere happens to meet the zone of influence of a bigger sphere, it does not stay rigorously inside the plane of assembling for a very long time. This behavior is more visible in the enlarged view of Figure 5. We distinguish very close to the biggest spherulite two small spherulites (indicated by arrows) which do not stay in focus, swinging up and down in the cell close to the bigger spherulite. The transport of the particles in the bulk of the cell is not likely to be a pure random Brownian motion because their fluctuations are no longer purely thermal. The succession of panels of Figure 5 shows that the aggregate is not rigid in space, and that the fluctuations of the particles around an average position is greater for the smaller particles. We also notice that the bigger spheres are farther from each other than the smaller spheres.

3.1.2 Influence of the electric field strength on the assembling dynamics and density

The influence of the AC field amplitude on the aggregate structure is illustrated in Figure 6. The pictures have been chosen at a later stage of the aggregation process, when the number of layered particles is quasi-stationary. These experiments have been performed with the same spherulite and copper sulphate concentrations. The density of layered particles clearly increases with the electric field. To quantitatively confirm this observation, and to further analyze the effect of the field on the assembling, a specific analyzing algorithm was elaborated.

The noisy character of the particle assembly pictures makes their quantitative analysis rather complex. A direct Fourier analysis can hardly differentiate between particles in and out of focus; as shown in Figure 7b, it is quite impossible to extract their characteristic sizes since moreover they are polydispersed. For getting round this difficulty, we have used a space-scale analysis to detect circular objects with different sizes from two-dimensional digitized

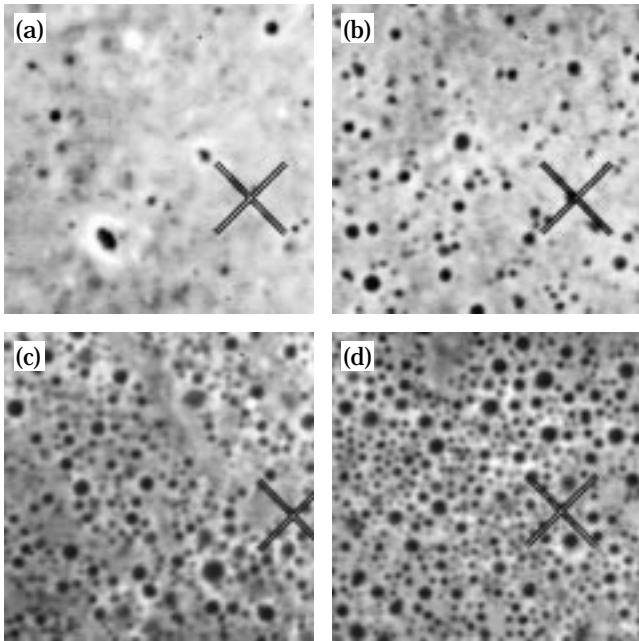


Fig. 6. AC field dependence of the (frequency 1 kHz) assembly of spherulites. (a) $E = 0$ V/cm, (b) $E = 100$ V/cm, (c) $E = 150$ V/cm, (d) $E = 225$ V/cm. Width of the pictures $30 \mu\text{m}$.

pictures [24]. The result of this computation is shown in Figure 7c. We checked the robustness of our detection algorithm by varying the detection threshold and we found a whole interval where the temporal behavior of the number of particles assembled close to the electrode is invariant. This automatic detection of spherulites brings a definite improvement of our experimental technique. We must nevertheless note that this image analysis slightly reduces the spatial resolution of our phase contrast microscope since it is limited to particle diameters greater than $1 \mu\text{m}$.

This algorithm was used to build Figure 8 which reports the temporal evolution of the layered spherulites for different AC field intensities. It confirms the optical observation in Figure 6 of the increase of layered particles with respect to the AC field amplitude. Moreover, this Figure 8 shows that the kinetics of the assembling process speeds up with the AC field amplitude. At 225 V/cm, it takes only a few seconds to get a quasi-stationary assembling of particles which explains why we don't show this evolution in Figure 8a; we can simply measure the average number of particles $\sim 1000 \pm 50$. The two curves correspond respectively to 100 V/cm (squares) and 150 V/cm (three branch stars) and provide evidence for two subsequent temporal regimes in the assembling process. A first regime (from 0 to ~ 100 s) which strongly depends on the field strength and a second regime which seems to be less dependent on the field intensity for this frequency of AC field forcing. The log-log plots of Figure 8b indicates that, in the second stage of the assembling process, the temporal behavior of assembled particles approaches a square root law of time, which could mean that at that stage, a diffusion-limited process is recovered. In the first stage, the limiting process is not the diffusion of spheru-

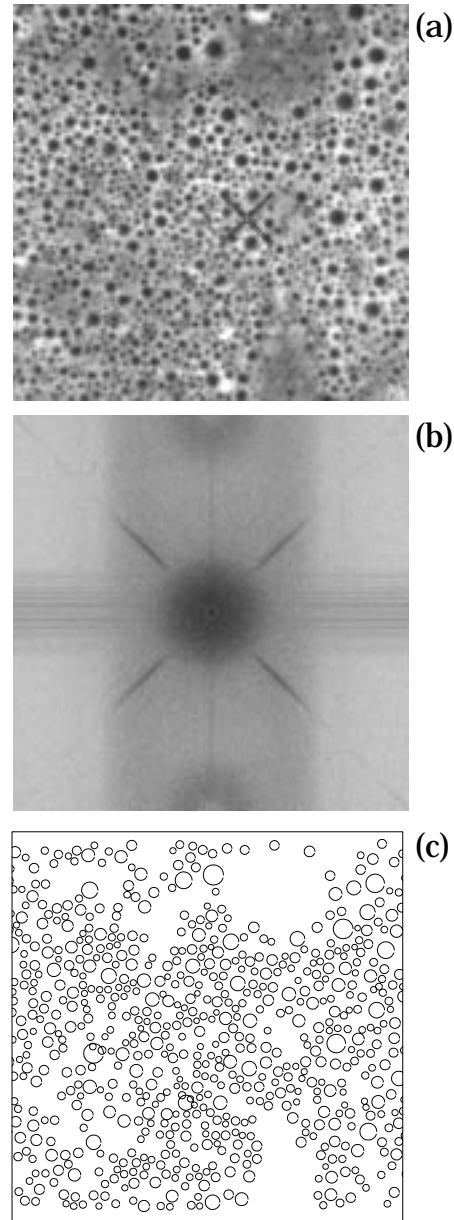


Fig. 7. Structural characterization of a spherulite aggregate. (a) Original picture, (b) Fourier transform of (a), (c) outlined contours of (a), as obtained with our detection algorithm.

lites from the bulk. This could be interpreted by the fact that the particles which are first attracted onto the surface belong to a “trapping” zone where there are accelerated by the electrostatic forces with the interface. Once confined in the plane of the electrodes, they self-organize into patchy zones by electrohydrodynamic forces (see below) while the density in spherulites keeps on growing by diffusion from the bulk, up to a stationary state where it no longer changes.

A deeper insight on the respective dynamics of the particles with respect to their size is straightforward thanks to our image analysis. In Figure 9, we show that the bigger spherulites [$2, 2.5 \mu\text{m}$] in diameter reach a quasistationary distribution after 150 s (bright squares), whereas the

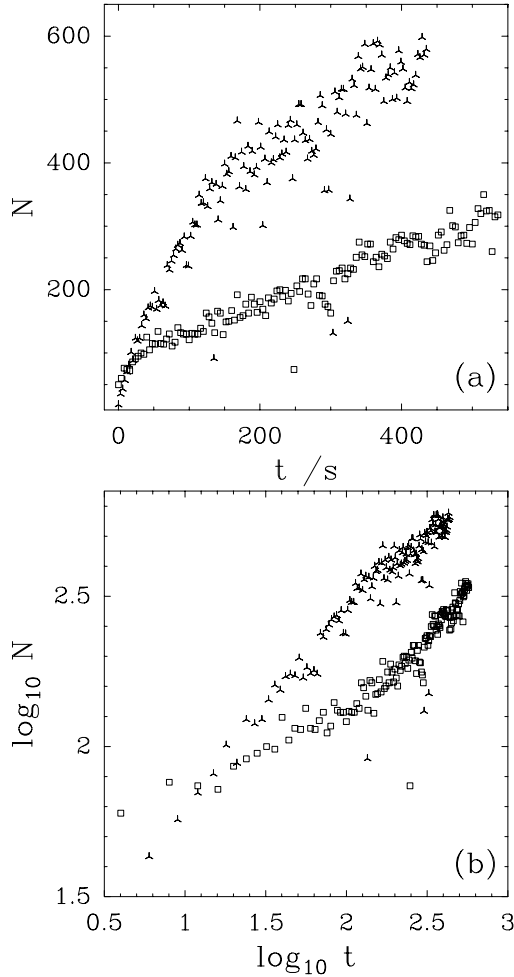


Fig. 8. Time evolution of the number of spherulites on the surface of the electrode for different amplitudes of the AC field during the aggregation process (three branch star: 150 V/cm, square: 100 V/cm, frequency 1 kHz); (a) lin-lin representation, (b) log-log representation.

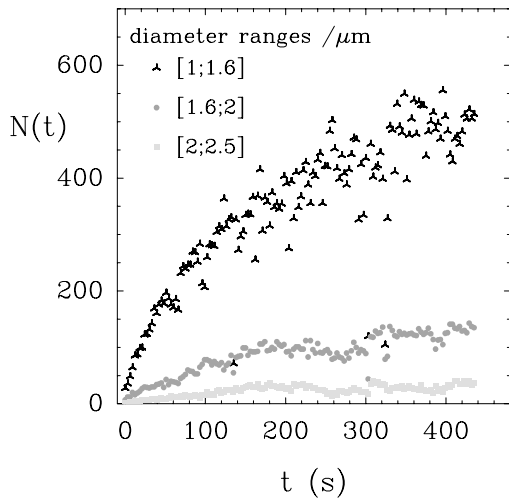


Fig. 9. Dynamics of the spherulite density *versus* time during the assembly process with respect to their sizes. AC field amplitude 150 V/cm, frequency 1 kHz.

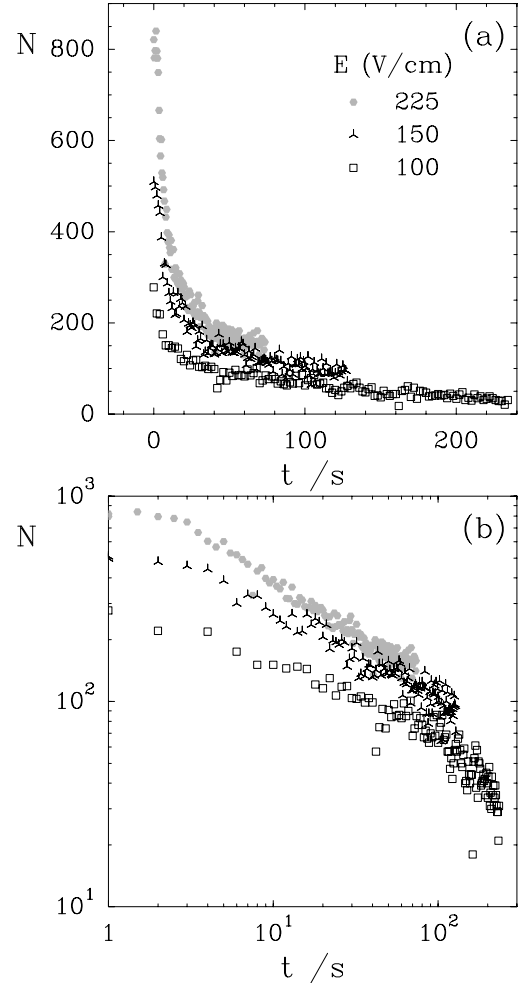


Fig. 10. Time evolution of the number of spherulites on the surface of the electrode for different amplitudes of the AC field during the dispersion process (frequency 1 kHz); (a) lin-lin representation, (b) log-log representation.

density of the smaller ones is still increasing after more than 400 s. We also notice that the fluctuations in the temporal evolution of the smaller particles are greater than those of the bigger particles, reflecting the enhanced wandering of these latter as guessed in Figure 5.

The redispersion of the layered spherulites does not depend on the amplitude of the AC field used for their assembling. This is evidenced in Figure 10a, where the time evolution of the number of layered spherulites during the dispersion phase is plotted. The three sets of data (100 V/cm, 150 V/cm, 225 V/cm) follow a $-1/2$ power law of time during the first 100 s, as shown in the log-log plot of Figure 10b. This can be understood by the Brownian character of the particles.

3.1.3 Influence of the frequency of the AC field on the assembling dynamics and density

The range of frequency where the spherulite response to AC field can be observed is rather narrow. The phase diagram of Figure 2 shows that it is limited from below, at

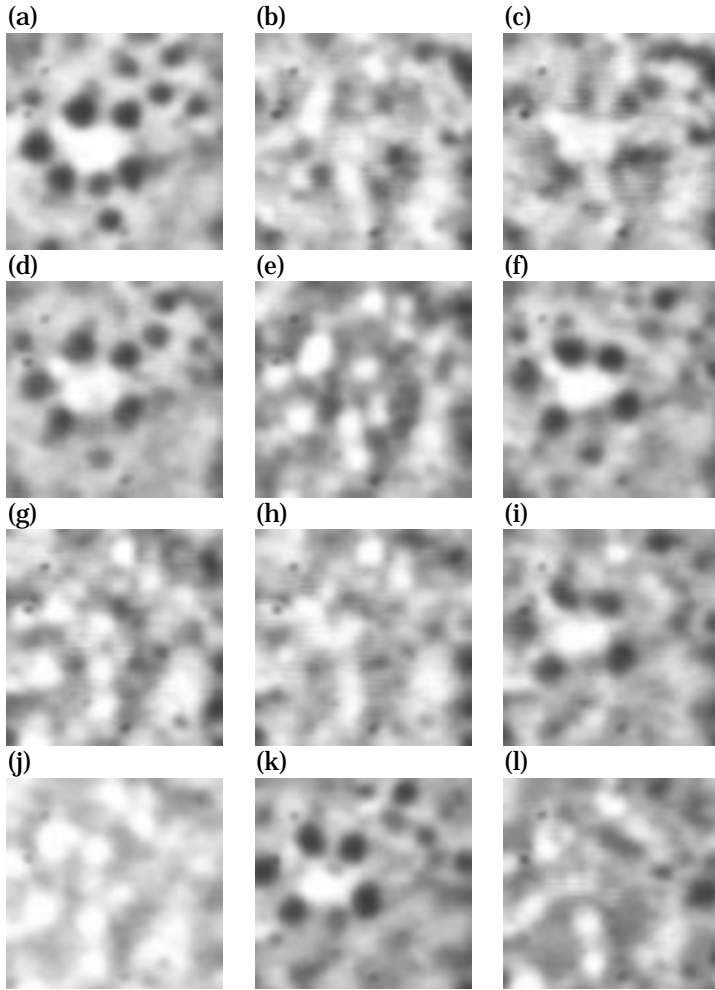


Fig. 11. Evidence of the pulsation of the fluid and the particles for a lower frequency field, time interval between successive pictures: $\Delta t = 0.05$ s, $\nu = 10$ Hz, $E = 150$ V/cm. Width of the pictures $10 \mu\text{m}$.

low frequencies, by the spherulite destruction by the AC field. Despite the spherulites are destroyed progressively by the AC field for frequency below 500 Hz, the direct video observation of the local dynamics of particles at low frequency is very helpful to understand the mechanisms underlying the assembling process. This is illustrated in Figure 11 for a 10 Hz forcing. At this frequency, despite we cannot conclude about the aggregation of particle, we see that both particles and their surrounding fluid undergo a global oscillation. Above 1 kHz, we have observed that the greater the frequency, the slower the aggregation process, and the smaller the density of aggregated spherulites, up to a point (around 100 kHz) where no aggregation was observed within 30 minutes. Let us note that the metastability of the spherulites in water prevents experimental studies beyond one hour since they are progressively stripped of their external bilayers which progressively cover the electrode and are likely to distort the current lines by dielectric screening.

3.1.4 Influence of the AC field on the size distribution of the layered spherulites

Figure 12 shows the superimposition of four distinct histograms of sizes, obtained respectively for three different

field amplitudes (100, 150, and 225 V/cm) at 1 kHz and for 350 V/cm at 20 kHz. It is immediate to recognize in Figure 12 that the increase of the electric field in the cell, at a given frequency ν , increases the total density of particles assembled on the electrode, as already discussed in Figure 8. A further result can moreover be extracted from this figure, when the electric field is increased, the rightmost part of the histograms (larger size particles) does not change much whereas the maximum of these distributions shifts towards smaller sizes. This observation brings the clue that the electric field can be used as a parameter for size selection, the higher field favoring the smaller size particles with respect to the bigger ones. The last histogram (20 kHz, 350 V/cm) is not less interesting since it illustrates the influence of the frequency of the AC field. We have chosen a much greater frequency for clarity of the demonstration. In this case, we could not detect a sufficient aggregation within one hour below 250 V/cm and we needed therefore to take a higher AC field. The important and unexpected features which are brought by this histogram are not only the fact that the density of particles decreases with the AC field frequency but also the fact that the distribution of sizes of aggregated particles is shifted towards the right, favoring the larger sizes.

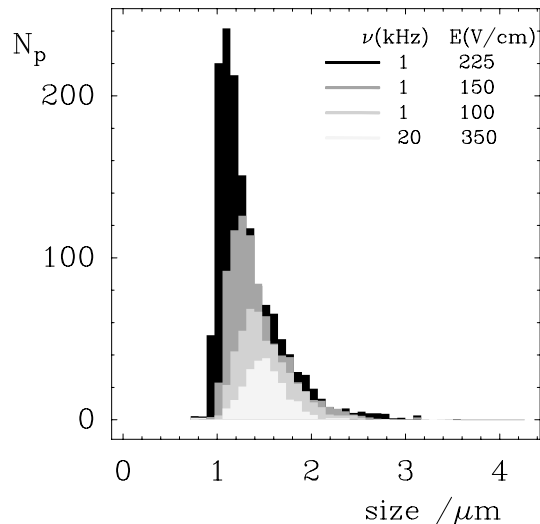


Fig. 12. Histograms of sizes of the assemblies of particles (in the quasi-stationary regime) for different AC field amplitudes and two different frequencies.

3.2 Discussion

The above study of the assembly of spherulites under AC field has revealed its complexity. We will try in this section to expose the physical mechanisms which govern the assembly process and to interpret our experimental observations.

3.2.1 Modeling of spherulites

A key property of our spherulites comes from the fact that they bear charges. They are not neutral and contain complexed copper cations (nitrogen and oxygen dipoles chelate the copper cations [21]) whose charges are compensated by sulfate anions either in the aqueous phase between the lipidic bilayers or in the aqueous phase surrounding the spherulite. A naive sketch of the charges of the spherulite is given in Figure 1a. If one assumes in a first stage that the inner ionic charges are isolated from the outermost charges by the stack of lipidic bilayers, one can model each spherulite by a sphere bearing a simple double layer on its outer shell.

3.2.2 Description of the interaction forces involved in the assembling process

In the process which leads to the formation of aggregated zones on the electrode planes, two types of interactions must be distinguished:

- (i) The particle-electrode interaction.
- (ii) The particle-particle interaction, once they are assembled on the surface.

The first interaction (particle-electrode), which is responsible for the two-dimensional (2D) layering of the

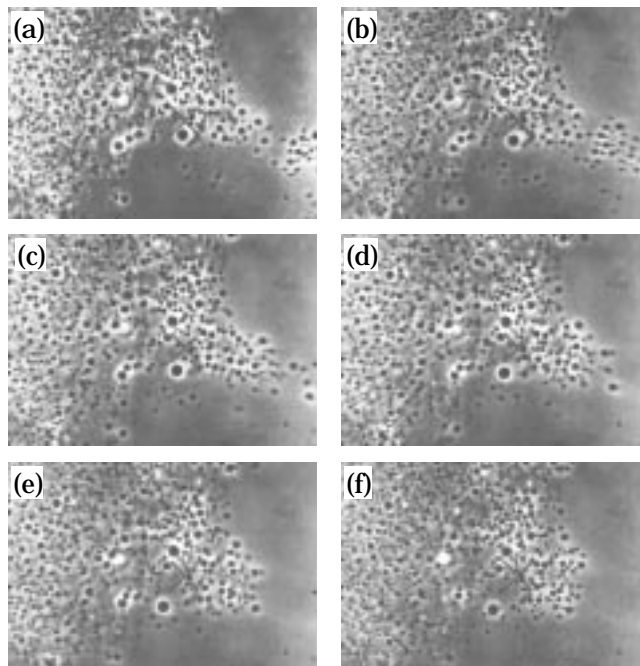


Fig. 13. Electrohydrodynamically induced drift of isolated particles towards an aggregation zone. The time interval between successive pictures is $\Delta t = 1$ s. Width of the pictures $20 \mu\text{m}$.

spherulites, can be described by two forces. One is electrostatic and attractive in both AC field alternances and results in the confinement of the particles on the electrode. This force is related to the polarization of particles by the electric field when they come close to the electrode. The greater the electric field and the charge distribution on the outermost shell of the spherulites, the stronger this attractive force. This interaction depends therefore on the size of the spherulites, the bigger they are, the greater their dipolar moment and the stronger the attraction with the electrode. When the electric field is increased the range of particle sizes which are trapped on the electrode is therefore extended to smaller sizes, as shown in Figure 12. This also explains why the global density of particles on the electrode increases (Fig. 8). The second force results from the electrophoretic displacement of the particle and tends to limit the distance of approach of the particles to the electrode. The local increase in charge distribution on the electrode surface when a particle comes close to it is likely to enhance the local pressure and to prevent the close stacking of the particle on the electrode [25].

The second interaction (particle-particle) reverses the respective signs of these forces. The electrostatic force between particles becomes repulsive and explains why the particles are not closely packed on the surface of the electrode. The bigger the particle, the greater its dipolar momentum and the greater its repulsion with respect to its neighbours. This can be noticed in Figures 4 and 5 where the interspace between the biggest spherulites is much larger than the distance between the smallest ones. The fact that patchy aggregated zones form on the

electrode reveals also an attractive force, which is of electrohydrodynamic nature. Simultaneously to the direct electrostatic attraction of the surface charges of both the particle and the electrode, a dielectric screening effect occurs which modifies the fluid streamlines both on the electrode and on the particle [1, 25, 26] and implies a fluid driving force parallel to the electrode. This global transport of the fluid is quite obvious when one studies the interaction of a big aggregate of particles with a smaller aggregate, as shown in Figure 13 by a small group of particles drifting towards a bigger cluster. On the edges of the particle clusters we invariably observe a global drift of the fluid which tends to attract the farther spherulites closer to them. This observation denotes two important properties, namely, the spatial extension of this interaction and the fact that there must be a component of the electric field parallel to the electrode. This electrohydrodynamic coupling between two different size groups of particles moves in priority the smaller group of particles.

3.2.3 Dynamics of the assembling process

The set of the interaction forces which has been described in the previous paragraph is likely to be a good basis for modeling. Nevertheless, it does not bring any information about the dynamics of the assembling process. The calculations which have been proposed by the past focus mainly on stationary solutions [1, 25, 26]. Since we work with pulsed current the characteristic settling time of each of these interactions must be included in our discussion as well as their strengths. We must stress the fact that the dynamics of the electrostatic interaction is much faster than that of the electrohydrodynamic forces.

To bring a clear picture of the time scales of the different interaction forces involved in the assembly process, it is necessary to distinguish by their characteristic frequency the successive field induced polarizations of the diffuse layer of both the particles and the electrodes. The simplest case corresponds to a planar surface which is submitted to a perpendicular field. The time necessary τ_d to reach a stationary charge distribution of the diffuse layer involves the displacement of charges on length scales of the order of the Debye length $1/\kappa$. In our solutions this length was estimated $1/\kappa \sim 7$ nm from conductance measurement of the ionic concentration (see below). From this value of κ , τ_d has been calculated $\tau_d = 1/(\kappa^2 D) \sim 5 \cdot 10^{-7}$ s (D is the diffusion coefficient taken equal to 10^{-6} cm²s⁻¹ for this computation).

The situation is more complex when the interface is curved as for example the spherulites. In this case, one can distinguish two successive processes. The first one which can be compared to the preceding diffuse layer building, leads to a fast distortion of the charge distribution around the particle (Fig. 14a to b). On the contrary to the planar case with a perpendicular field, this polarized particle (its bears a dipole) does not correspond to a stationary state. The second process produces an electro-osmotic flow on the lateral charges of the particles and enhances also the global polarization of the particle (Fig. 14c).

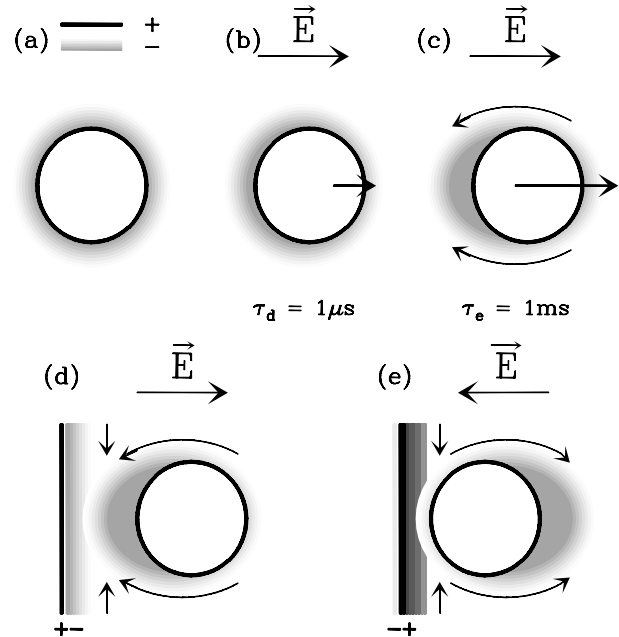


Fig. 14. Dielectric and electrohydrodynamic polarization of the surface charges when submitted to an electric field. (a) A single particle at equilibrium, (b) dielectric relaxation of a single particle, submitted to an electric field, (c) electrohydrodynamic polarization of a particle, submitted to an electric field, (d) and (e) electrode-particle polarizations under electric field. In each representation the stream lines have been drawn by hand to illustrate the electroconvective transport.

This phenomenon constitutes the basis of electrophoresis [27, 28]. This process takes much longer to settle. The characteristic relaxation time of electrophoretic polarization is typically $\tau_e \sim a^2/D \sim 10^{-2}-10^{-3}$ s, it is limited by the diffusion of charges on the length scale of the particle and increases with its size.

The characteristic time of the dielectric relaxation of the diffuse layer around the particle is confirmed by conductance measurements shown in Figure 15. The domain of frequency of this dielectric relaxation is rather narrow and centered around 2×10^6 Hz which shows that in our systems the charges are rather homogeneously distributed. For lower frequencies, no other effect can be detected by conductimetry which comes probably from experimental limitations due to the electrode charge transfer polarization, as shown in the Cole-Cole plot of Figure 15. Let us also remark that the DC value of the conductance of the dispersed spherulite phase is not negligible and shows a weak leaking ($\sim 10\%$) of the copper ions from the spherulites.

Let us consider now the polarization of an electrode in the presence of particles. In this case, the presence of the particle produces a dielectric screening of the electric field lines and inhibits the rapid polarization of the diffuse layer on the electrode because there is a breaking of the parallel symmetry of the field lines. Similarly to the case of a spherical particle embedded in an electric field, electroosmotic effects are also involved and the inhomogeneity of the field

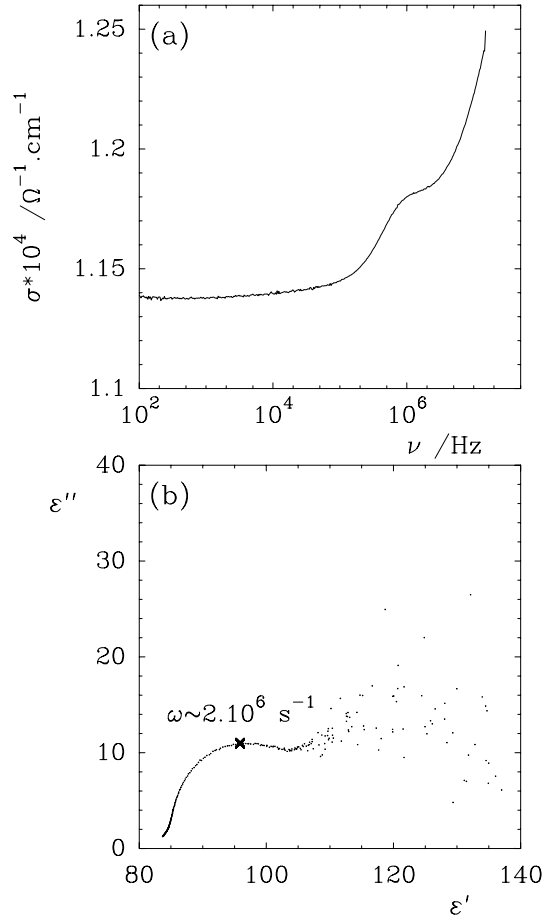


Fig. 15. (a) Lin-log plot of the conductance of the dispersion of spherulites *versus* frequency. (b) Cole-Cole plot of its dielectric relaxation. The composition is given in the experimental set-up section.

tends to sweep the fluid along the electrode towards the particles (Figs. 14d and e). The fluid streamlines and velocity of the electrophoretic flow around a non conducting particle in the neighbourhood of an electrode have already been computed by Fransaer [26] in the thin double layer approximation. Let us mention that in our experiments the thin layer approximation $\kappa a \gg 1$ (a is the diameter of a particle) is relevant. The situation in AC field bears some resemblance with this approach although it cannot be treated as a stationary process and our system involves also more than one particle interacting on the surface.

One can assume therefore that in the range of frequencies where the aggregation process has been observed (≥ 1 kHz), the radial diffuse layer relaxations on the spherulite interfaces are fast enough to adjust themselves to their electroosmotic distortion by tangential fields. On the contrary, the tangential diffusion of charges which generates the electroosmotic transport might be shortened by AC field frequencies above 1 kHz and therefore its electroosmotic distortion prevented. As a consequence, their dipolar momentum might be reduced, as well as the attractive interaction between the charges of the particle and those of the electrode. This effect is reflected in the

decrease of the density of layered particles with respect to frequency in Figure 12.

As far as the size distribution and dynamics of particles are concerned, one should expect the smaller particles to respond at higher frequencies than the bigger ones since the smaller the spherulites, the smaller τ_e . It is not exactly what is reported in Figure 12, since higher frequencies select bigger size particles. The strongest attraction of the bigger particles on the electrode is likely to be related to their greater size and greater charge. The electrostatic interaction of the smaller particles with the electrode is weaker, which explains why they do not stay steady in the plane of assembly (Fig. 5). Moreover, during the first stage of the aggregation process the attraction between the spherulites and the electrode is strong because the surface of the electrode is still free of spherulites. When the density of spherulites layered on the electrode increases the charging process of the electrode is progressively slowed down and the attractive force is damped. When the AC field frequency is increased this charging gets progressively inefficient which explains why the smaller particles are no longer attracted because their attraction is too weak.

To conclude this discussion, we would like to note again some fundamental issues that have been raised by our experimental study and which should be recorded in the modeling of these processes:

- the permuted roles of the antagonist electrostatic and electrohydrodynamic forces of particle-particle and particle-electrode interactions;
- the differentiation of the dynamics of the particles and the electrode when submitted to an AC field and the role of the size of the particles on the building of the diffuse layer;
- the nonstationary modeling of the dielectrophoretic transport to account for transitory effects and explain the two successive stages of the aggregation process;
- the possibility of size selection with a careful choice of both AC field amplitude and frequency.

With respect to our multilamellar vesicles, additional interrogations have appeared, in particular those concerning their intrinsic stability under AC field and their possible deformation close to the electrode. The richness of these spherulites for surface treatment purposes makes them nevertheless deeply attractive despite their increased complexity. Such applications are actually under progress in our laboratory.

We are very indebted to F. Gauffre and D. Roux for revealing us the recipes for the spherulite formulation and for fruitful discussions. We are very grateful to S. Regnault and C. Coulon for their help in conductance measurements. We want to thank also A. Ajdari, A. Arneodo and J.F. Muzy for stimulating discussions. One of us (C.F.) acknowledges a financial support from a FEDER grant.

References

1. S. Yeh, M. Seul, B. Shraiman, *Nature* **386**, 57 (1997).
2. P. Pieranski, *Phys. Rev. Lett.* **45**, 569 (1980).
3. D. Chan, J. Henry, L. White, *J. Colloid Interf. Sci.* **79**, 410 (1981).
4. H. Deckman, J. Dunsmuir, *Appl. Phys. Lett.* **41**, 377 (1982).
5. G. Onoda, *Phys. Rev. Lett.* **55**, 226 (1985).
6. S. Hayashi, Y. Kumamoto, T. Suzuki, T. Hirai, *J. Colloid Interf. Sci.* **144**, 538 (1991).
7. N. Denkov, O. Velev, P. Kralchevsky, I. Ivanov, H. Yoshimura, K. Nagayama, *Langmuir* **8**, 3183 (1992).
8. C. Dushkin, H. Yoshimura, K. Nagayama, *Chem. Phys. Lett.* **204**, 455 (1993).
9. P. Kralchevsky, V. Paunov, I. Ivanov, K. Nagayama, *J. Colloid Interf. Sci.* **151**, 79 (1992).
10. P. Kralchevsky, K. Nagayama, *Langmuir* **10**, 23 (1994).
11. A. Dimitrov, K. Nagayama, *Langmuir* **12**, 1303 (1996).
12. P. Richetti, J. Prost, P. Barois, *J. Phys. Lett.* **45**, 1137 (1984).
13. M. Giersig, P. Mulvaney, *J. Phys. Chem.* **97**, 6334 (1993).
14. M. Trau, D. Saville, I. Aksay, *Science* **272**, 706 (1996).
15. C. Dushkin, T. Miwa, K. Nagayama (unpublished).
16. D. Saville, *Ann. Rev. Fluid. Mech.* **9**, 321 (1977).
17. R. O'Brien, *Adv. Colloid Interf. Sci.* **16**, 281 (1982).
18. J. Anderson, *Ann. Rev. Fluid. Mech.* **21**, 61 (1989).
19. O. Diat, D. Roux, *J. Phys. II France* **3**, 9 (1993).
20. O. Diat, D. Roux, F. Nallet, *J. Phys. II France* **3**, 1427 (1993).
21. F. Gauffre, Ph.D. thesis, Université de Bordeaux I, 1997.
22. F. Gauffre, D. Roux, submitted to *J. Chem. Phys.* (unpublished).
23. Data Translation frame grabber (768×512) and public domain NIH Image program, developed at the U.S. National Institutes of Health and available on the Internet at <http://rsb.info.nih.gov/nih-image/>.
24. T. Lindeberg, *Scale-scale theory in computer vision* (Kluwer Academic Publishers, Dordrecht, The Netherlands, 1997).
25. F. Morrison, J. Stuckel, *J. Colloid Interf. Sci.* **33**, 88 (1970).
26. J. Franssaer, Ph.D. thesis, Katholieke Universiteit Leuven, 1994.
27. R. Hunter, *Zeta potential in colloid science* (Academic Press, London, 1981).
28. R. Hunter, *Foundation of colloid science* (Clarendon Press, Oxford, 1986).